A FLOW FIELD AROUND A CYLINDRICAL PROBE IN PROXIMITY TO STATOR BLADES AND ITS EFFECT ON THE MEASUREMENTS

Viacheslav A Sedunin **Liping Xu** **Ilya A Kalinin** **Iurii G Marchenko** **Oleg V Komarov**

Whittle Laboratory University of Cambridge, Cambridge, UK

Energy Institute
Ural Federal University Yekaterinburg, Russia

ABSTRACT

In multistage axial compressors of gas turbine engines there is a need for a detailed understanding of the flow field in between the blade rows, which could be obtained by spanwise traversing. This requires a pneumatic probe to be immersed into the flow path between the blade rows, where the space is limited. Therefore, the probe will affect the flow field around it and in the blade channel, and the probe readings will be affected by that flow field. As a result, these probe readings cannot be translated to flow parameters based on just the freestream calibration characteristics, obtained in the idealized wind tunnel.

In our paper, we provide a computational analysis of the flow field around the cylindrical probe in a constrained inter-blade-row environment at different circumferential locations and flow conditions both upstream and downstream of the stator blade row. It is shown that the flow angle measurement error can reach up to five degrees in the mid-pitch locations compared to undistorted flow, and dynamic head measurements can be up to 30% away from the actual mean values of the flow. These deviations are shown to be caused by flow field interaction inside the blade channel and, as a result, measured values, obtained during industrial compressor testing, could be corrected accordingly. The universal correction procedure is proposed for further use in the industry.

NOMENCLATURE

CFD computational fluid dynamics;
CFX CFD solver from ANSYS;
RANS Reynolds-averaged Navier–Stokes;
SST shear stress transport turbulence model;
Cp non-dimensional pressure coefficient;
p pressure;
φ yaw angle/ ΔFlow angle;
y+ nondimensional distance from the wall;
SS suction surface;
PS pressure surface;
LE leading edge;
TE trailing edge.

INTRODUCTION

Nowadays the axial compressor design process in many companies is largely based on the methods of computational fluid dynamics (CFD). This includes two- and three-dimensional optimization of the blade channels, consideration of fluid-structure interaction, and then matching compressor stages into one flow path. Unlike the traditional approach, where experimentally based correlations were used at each step of the process, in the simulation-based approach, the experimental data is usually available only when the full-scale demonstrator or even the pilot gas turbine engine is manufactured. The latter case is more relevant for heavy-duty gas turbines, especially during modernization and retrofit. For the computationally based approach, it is vital to have refined measurements of the actual flow field in the whole compressor, as this can be used for necessary tuning and can be fed back into the design system.

Experimental study of the full-speed machine brings more instrumentation challenges and more measurement uncertainties than low-speed laboratory-scale compressors. This is especially true when spanwise flow measurements are required. The key reasons for that are limited axial spacings between the blade rows, high flow velocities (although, subsonic for most of the stages), and multiple constraints outside the compressor casing, which leaves only certain circumferential positions for the traversing mechanisms to be set. On top of that, when compressor retrofit is desired, the blade count can be changed together with the radial stacking of three-dimensional blades. Therefore, the pneumatic probe location inside the compressor flow path is far from ideal, and the question arises about how this location and the flow conditions affect the probe's readings.

To answer this question, we analyze the flow field around the cylindrical probe when in proximity

to the stator blades, and how this affects the readings. This probe together with its holding stem causes significant blockage and flow re-distribution in the blade channel. The current paper addresses the flow field interaction from the point of view of the probe itself and its interpretation of the flow parameters, rather than the probe's effect on the blade row performance.

Traditionally, this probe would be first calibrated in the steady and homogeneous flow of the laboratory calibration tunnel, and then calibration coefficients from this idealized environment would be used to process the raw experimental data. In the paper we show that these coefficients are no longer valid for the constrained blade channel, and appropriate corrections should be applied as a function of the pitchwise position of the probe, and the freestream Mach number.

There are multiple published research materials on spanwise traversing in axial compressors, normally carried out at low-speed rigs with one or two stages (see, for example, [1,2]). The low speed and the large dimensions of the rig allow for better spatial and time resolution of the measurements and a wider range of experimental methods, including hot-wire anemometry, and oil-flow visualization, which are rarely available at the full-speed machines on-site. Lakshminarayana et al (1996) carried out a similar approach to the compressor with a tip Mach number of 0.5, but the rig was intentionally made for research purposes with sufficient axial gaps and possible pitchwise motion of the probe, so the spanwise distributions were obtained as pitchwise averaged values at each immersion distance, and no corrections were applied to the measured values.

For industrial testing due to mechanical constraints and space limitations, the circumferential motion of the probe is no longer possible, as this will require wide circumferential slots on the casing of the industrial machine in operation, and these slots can significantly affect the structural integrity.

But even when the probe is immersed radially downwards, for high-speed compressors the situation becomes more complicated when the probe holder bends due to significant aerodynamic load, and the probe is pushed further downstream – either inside the stator blade channel or towards downstream rotating blades with a risk of impact.

Research into the probe's impact on compressor performance has been studied deeply and is well represented in the literature. Coldrick et al (2003) and (2004) present an extensive study on using pneumatic probes in high-speed axial compressors. The authors found that pressure and velocity fields in the region between the blade and the probe are distorted, leading to an erroneous reading on the adjacent probe pressure ports. Coldrick claims approximately 3.3 degrees of total uncertainty. However, the authors propose to resolve this uncertainty by moving the probe away from the centre of the passage without giving estimations on how far the probe should be moved, nor do they explain the flow physics to quantify the movement.

For the four-hole probe Coldrick et al (2004) reported a very minor difference between undisturbed flow parameters and that with the probe immersed. It was also concluded that any flow angle error in measurements arises because the entire pressure distribution around the probe is shifted, rather than an error appearing in an individual hole reading.

The impact of the immersed probe and its holder on the compressor performance was investigated by Seki et al (2021). The immersed structure caused up to two per cent growth of the total pressure at the stator inlet, although the immersed stem was significantly larger than the probe and it introduced considerable blockage to the passage. The authors do not discuss, however, the effect of the flow change on the probe's readings.

To the best of our knowledge, there exists no published study of the cylindrical probe reading correction due to its proximity to the stator blades, and therefore, it is unclear how to approach implied measurement uncertainties during the experimental study depending on the geometrical and flow parameters. To address this, the paper explores the impact of the potential flow fields effect of both the blades and the cylindrical probe on each other. Emphasis is placed on understanding the fundamental flow features caused by the presence of such a probe. It is shown that the blade vicinity effect on probe readings in high-speed compressors is greater than usually thought, and near the blades, the uncertainty of probe readings is highly non-linear.

To illustrate this problem, Figure 1 shows integrated mass flow values, calculated based on spanwise traversing at several axial locations of the 10-stage industrial compressor. The obtained values vary between 94 and 112% of that measured at the compressor inlet. This was found to be caused by large uncertainties in the dynamic head and the flow angle measurements, which then propagate to axial velocity calculations and density, and then – the calculated mass flow. An investigation of the possible reasons for such uncertainties and the ways of mitigating them led to the present paper.

When corrections were applied mass flow readings at all sections fell within four per cent of the inlet value, which is still reasonably high, but can further be explained by larger uncertainties in end-wall measurements.

The remainder of the paper is structured in the following way: first, the research compressor is presented together with the challenges met. Then, basic mechanisms affecting the flow around the cylinder in a constrained environment are studied, followed by a series of CFD experiments with varying probe positions and flow conditions. Lastly,

the data analysis leads to the correction of the raw experimental data, which has shown significant improvement in the consistency of the measurements along the compressor flow path at different operating points.

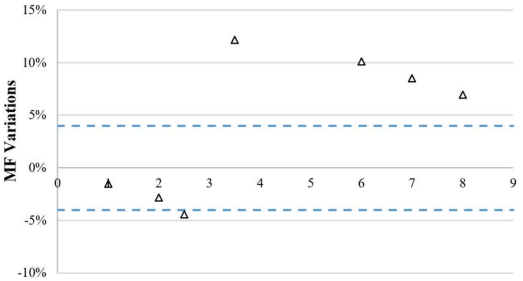

FIGURE 1: INTEGRAL MASS FLOWS AT EACH TRAVERSING SECTION OF THE INDUSTRIAL COMPRESSOR COMPARED TO THE INLET MASS FLOW AT DESIGN CONDITION

METHODS

The present work uses CFD simulations of the representative flow conditions to understand the impact of the constrained multistage environment on the measurement uncertainties of the pneumatic probe. First, the industrial compressor of interest is described together with the probe used in the study, followed by the modelling parameters and the range of geometrical variables.

The research compressor

The research compressor was instrumented and prepared as a module of an industrial gas turbine engine, which allowed measurements to be taken along the operating line matching the turbine performance. The concept of the research gas turbine power plant is similar to the one described by Mito (2015) and was adopted as a test engine to acquire various component data through special measurements taken during trial operation.

The compressor has subsonic inlet and frontal stages, yet it has relatively high loading coefficients between 0.32 and 0.37 at midspan which are representative of modern industrial machines. The sketch of the compressor cross-section is presented in Figure 2 with the traversing sections marked in red. Relatively high loading coefficients and the presence of significant separation zones were considered an opportunity to improve compressor efficiency and part-load operating stability using the 3D RANS simulations and implementation of 3D blading. This is why one of the GT engines was prepared for extensive experimental study before and after the re-blading as a part of the modernization project.

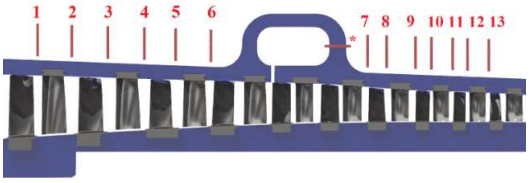

FIGURE 2: COMPRESSOR CROSS-SECTION WITH TRAVERSING LOCATIONS BETWEEN THE BLADE ROWS

For the current work the casing holes, originally made for the static pressure readings similar to the ones mentioned in Takuya et al.(2012) were used to immerse the cylindrical probe on the stainless steel solid cylindrical rod inside the compressor flow path.

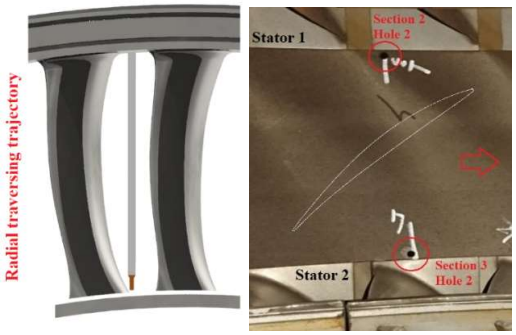

FIGURE 3: TRAVERSING TRAJECTORY AGAINST THE SWEPT STATOR BLADES AT THE INLET (LEFT) AND VIEW ON CASING HOLES DOWNSTREAM OF STATOR 1 AND UPSTREAM OF THE STATOR 2 (RIGHT) (CONTOUR OF A ROTOR BLADE IS SHOWN FOR REFERENCE)

In contrast to research compressors at the laboratory scale, real gas turbine engines would have multiple external structures and mechanisms, attached to the compressor casing. Elements like blow-off valves, casing enforcement ribs, air extraction collectors and pipes, IGV heating, and auxiliary air pipes will act as obstacles to the traversing equipment. The horizontal split flange and the presence of an even more complicated oil tank and pipes under the engine leave only the top half of the casing available for instrumentation.

Other factors include limited axial spacing between the blade rows, especially when the probe stem is bent by aerodynamic forces. Since the engine operates at high pressures and temperatures, there is a limitation to the traversing hole dimensions as well as the number of holes available.

Cylindrical multi-purpose probe

The three-hole pneumatic probe used for the traversing was also designed for temperature measurements (Figure 4). Initially, the design was

taken from Kupferschmied (1998) with the angle between side holes set at 42 degrees.

A cylindrical shape was chosen due to limited axial space between the blade rows and due to the uniform flow field around the probe regardless of its orientation, whereas for any non-axisymmetric type of probe the orientation would have brought another degree of uncertainty in the combined flow field effect. The cylindrical type shows good aerodynamic behaviour and minimal influence on the flow field, although this shape is less stable at the high Mach number flows.

Alternatively, for spanwise measurements of the compressor flow field, Kiel probes can be mounted on the stator leading edges. However, this method has limited resolution in a radial direction and does not provide information about the flow angle and its velocity. It also requires a proportional increase in the number of sensors and manual labour for instrumentation.

The probe has three pressure holes on one plane (position 1 in Figure 4). The concept of a combined temperature and pressure probe, although developed independently, is similar to Ashenbruck (2015) with a stagnation chamber (3) under the three holes. The chamber has a ventilation hole at its back, and since the area ratio of this hole to the chamber is around 50, the pressure in this chamber can be treated as the stagnation pressure of the flow. This feature was used for measurement reference in the experimental study and shown as (6). The probe is fixed in the stem with a thread (2) and all the hypodermic tubes are connected axially (4), it also has a safety contact wire at the probe's tip (5) to inform about the contact between the probe head and the rotor hub. The key geometrical parameters of the probe and the blade row are presented in Table 1.

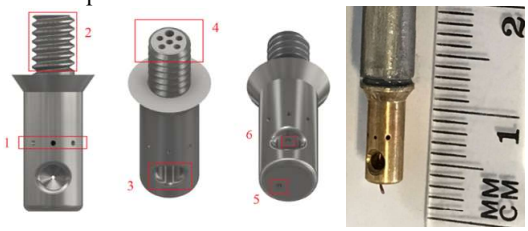

FIGURE 4: CYLINDRICAL PROBE WITH THREE HOLES AT 42 DEGREES (1), THREADED TIP (2) WITH HOLES (4) FOR HYPODERMIC TUBES AND THE THERMOCOUPLE, STAGNATION CHAMBER (3), SECURITY WIRE (5)

CFD modelling

Five stationary blades were considered for the computational study of the blade row, and the probe was immersed between blades 2 and 3, counting in direction of rotation. Rotating blades were not included in the study since the real probe was expected to measure a time-averaged signal

Parameter	Value	Unit
Blade type	NACA65	-
Flow turning	20	[deg]
Incidence range	-5 - +5	[deg]
Inlet Mach number	0.5 - 0.75	-
Probe diameter to blade pitch	4 - 8	[%]
LE thickness to blade pitch	3 - 8	[%]
Axial distance between the probe centre and the LE	1 - 3 d_{probe}	-
Angle between probe side holes	42	[deg]
Hole diameter to probe diameter	0.08 - 0.12	[mm]

TABLE 1: BLADE ROW AND PROBE PARAMETERS

The domain inlet has a uniform flow with a given direction and total pressure. The static pressure at the outlet was prescribed to control the inlet Mach number. ANSYS CFX flow solver was used with the default SST turbulence model and appropriate mesh resolution on the blade and probe surfaces with $y+ < 5$. Even though the flow distribution around the blade leading edges is primarily of an inviscid nature, the Cp distribution around the cylindrical probe depends on the boundary layer modelling with the transition from a laminar to a turbulent state. A Gamma-theta transition model has shown a good agreement with the calibration data and was further used for the presented study.

Several axial planes were chosen (Figure 5) to immerse the probe. Plane 0 is the one near the domain inlet and has a circumferentially uniform flow. Planes 1 and 2 are the actual positions of the immersed probe: Plane 1 represents the probe near the casing, where it just enters the flow path, however, when the probe is immersed radially further down, approaching the hub region, it is being pushed by the aerodynamic forces towards the blades – and this is where Plane 2 is drawn. Plane 3 was chosen at the hole locations downstream of the blade row. Due to the lower dynamic head, the stem is not expected to bend too much downstream for this location.

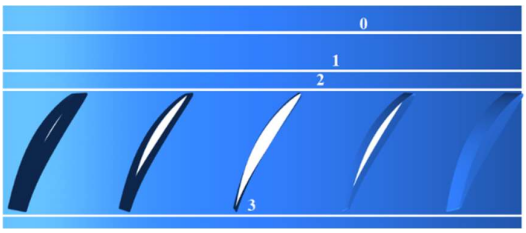

FIGURE 5: COMPUTATIONAL DOMAIN OF FIVE BLADES AND THE PROBE LOCATIONS AT THREE AXIAL PLANES

For the sake of simplicity, a smooth cylinder without pneumatic holes was simulated as a probe head in this study. Previous experience has shown a good agreement between pressure readings inside properly meshed and simulated holes and the values on the cylindrical surface of the probe at the same angular position. Also, to avoid tip effects, the cylinder went all the way through the computational domain. In the spanwise direction, the minimum feasible span height was set, so the problem can be considered quasi-two-dimensional. The cylindrical channel end walls were defined as free slip walls.

The same smooth cylinder of the probe was first calibrated in a freestream channel, as shown in Figure 6. This computational model was also used to study the effects of downstream contraction and proximity to walls on the pressure distribution around the cylinder, as will be shown in the next section.

UNIFORM FLOW IN A CONSTRAINED CHANNEL

When the probe is immersed in the flow channel, the flow around it is largely affected by the type of the boundaries and their proximity. This section aims to study these effects on the performance of the cylindrical probe. It starts from an unconstrained flow environment, typically used for laboratory calibration, then considers the channel with no-slip walls followed by the case where the probe is approaching one of the walls (Figure 6).

Figure 6 (b) shows the Cp distributions around the cylinder, which can be used to build calibration curves during the real experimentation process. The width of the channel and the positions of the probe were chosen to replicate the proportions of the region in front of the stator blades in the experimental compressor.

First, the calibration was simulated with the so-called, opening boundary condition at sidewalls, which allows the flow to enter and leave the domain on sides depending on wall pressure distributions. This means that when the probe introduces blockage, the flow can freely go around as it would do during the calibration in the freestream jet of the calibration tunnel. This case is referred to as the "No walls" case in Figure 6. Later in the paper this case is used as a reference "CFD freestream calibration" curve, and the calibration curves from that case are used to post-process probe "readings" into the flow parameters. This calibration was done for the whole range of inlet Mach numbers studied.

The Cp values are calculated as follows:

$$C_p = \frac{\left(p_s - \overline{p_{s,o}}\right)}{\left(\overline{p_{o,o}} - \overline{p_{s,o}}\right)} \quad (1)$$

Where $\overline{p_{o,o}}$ is a mass flow averaged total pressure and $\overline{p_{s,o}}$ is an area-averaged static pressure both at the domain's inlet. And p_s is a local static pressure at the probe's surface.

Then free-slip no penetration walls were introduced first, then the no-slip no penetration walls (Figure 6 (b)). The probe blockage has caused the flow acceleration in the channel, so the minimum Cp values are about 7% lower than that of the freestream jet. The difference in the side walls' boundary layers did not bring significant change in this case, so both lines overlap and are referred to as case 2.

Next, in case 3 the flow contraction was introduced at the same axial position as the probe's centre. It is representative of the flow contraction between the stator inlet plane and the throat of the channel. Here the minimum Cp value is lower by almost 10% of that of the freestream calibration.

For cases 4 and 5 the probe is placed at 10% of pitch aside from one of the walls. For case 4 the probe is experiencing non-uniform pressure distribution on the sides. As a result, if the freestream calibration coefficients were used, the probe readings would give up to 5° of flow incidence, despite the real flow angle throughout the channel being still zero (the flow is strictly vertical). This illustrates how the probe readings could be affected by local flow asymmetry and flow redistribution and could provide false angular measurements, which differ from the flow angle of the undisturbed channel.

Local flow distortion causes a shift of the stagnation point on the cylinder surface, which would normally be zero at the freestream calibration. The stagnation point is shifted by 2.7o away from vertical when the probe is in proximity to the sidewall.

Red lines in Figure 6 show the Cp distribution for case 5 – probe proximity to the wall with passage contraction downstream of the probe. The measurement error of the probe reading, in that case, would be up to 10o, and the stagnation point is shifted by 5.9°.

The angular position of the stagnation point on the cylindrical surface reflects the change in the flow angle around the probe. However, it does not mean that the probe reading will only be affected by the incoming flow – it will also be affected by the flow asymmetry around the probe. Therefore, the corrections for the two branches of red and blue lines in Figure 6 (c) can be made to decouple the effect of incoming flow angle change and the asymmetry of the flow around the probe. An example of that can be seen in Figure 7, where two branches of the Cp distributions already shifted according to the angular position of the stagnation point, but there is still a gap between the two lines, which shows the flow asymmetry. The effect of the flow asymmetry on the probe reading also will depend on the angular position of the side holes and the difference between

the central hole angle and that of the flow (Figure 7 top).

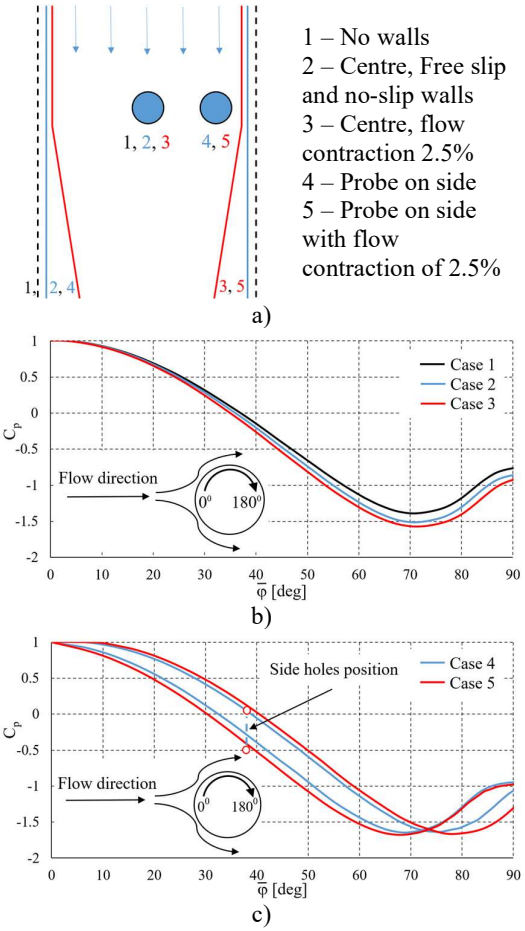

FIGURE 6: CALIBRATION DOMAIN WITH VARIABLE BOUNDARY CONDITIONS ON SIDES (a) AND VARIABLE FLOW CONTRACTION DOWNSTREAM FOR THE PROBE IN THE CENTER (b) AND NEAR THE WALL (c)

It is important here to define the ways of measuring the flow angle and the way it should be referred to either the averaged or local values of the flow (see Figure 7 for reference):

- Mass flow averaged flow angle at the inlet section away from the blades (Plane 0). This is the most important value for the multistage design system and experimental study, as this can be treated as a pitchwise averaged value at a given spanwise location.
- Local flow angle of undisturbed flow (no probe immersed) taken at the axial locations upstream and downstream of the blade row, where the probe will be placed later. This value is important as it could be easily gathered from the CFD simulation and then compared to locally measured value or converted to the pitchwise averaged one.
- Angular position of the stagnation point on the probe's cylindrical surface (see Figure 7 top for reference). This value will be different from the undisturbed flow local angle due to the flow field distortion.
- "Measured" flow angle – the one that will be obtained after processing the three pressure readings at the given angular positions of the cylinder.

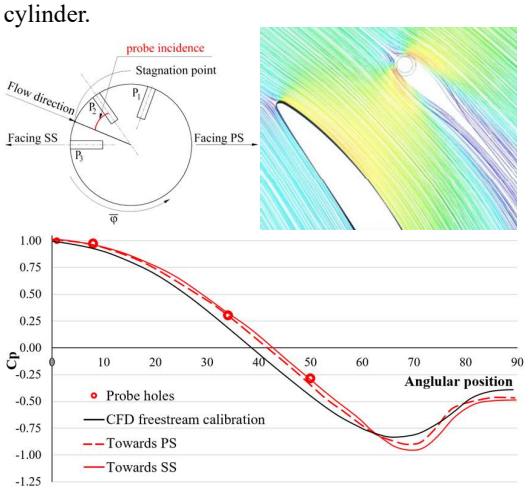

FIGURE 7: SCHEMATIC REPRESENTATION OF THE FLOW ANGLE MEASUREMENTS AROUND THE PROBE (TOP) AND THE Cp VALUES DISTRIBUTION (BOTTOM)

Since the probe's angular position around its axis is not varied during the traversing, the flow parameters must be calculated for any flow angle relative to the probe (within the calibration interval). Therefore, if there is a local acceleration on one side of the cylinder due to the blade surface proximity, the probe will see it as a different flow angle with further implications for raw data processing. In the current simulation the angle between the P2 hole and the circumferential direction of the blade row was set at 45°.

For a cylinder of relatively high diameter, there can be a significant flow asymmetry on the sides. The side of the probe towards the pressure side of the neighbouring blade sees separation further downstream compared to the opposite side of the probe (the one towards the pressure side of the next blade). The starting point for both lines is the stagnation point on the probe's surface. So, when the pressure is measured at three "holes" at 42o offset from each other (red points in Figure 7) the readings will show a slightly different yaw angle than that of the stagnation point. This difference was reaching 5-7o when the probe was approaching the blades.

RESULTS

This section provides the results of CFD simulations of the probe upstream and downstream of the stator blades. The corrections to the measured values are presented here in the same order as the

real data was processed during the experiment (taken from [15]). First, the yaw angle shall be defined, followed by the total pressure and then the dynamic head, hence, static pressure. In the end, a similar sequence is discussed for the CFD probe readings downstream of the stator blade row.

Flow angle

Figure 8 (a) shows the pitchwise distribution of the flow angle at two axial locations (see Figure 5 for reference location). Flow angles at various Mach numbers are in Figure 8 (b), and at various incidences in Figure 8 (c). The undisturbed local pressure values are shown in lines and probe readings are in symbols.

For these conditions the flow angles vary between -10 o and +6o, where "0" means the mass-flow averaged value at a given axial location. Values below zero here shall be interpreted as if the flow is moving less in the axial direction and more – in the circumferential. In terms of the blade row, such negative values on the graph would indicate a "positive" incidence and, therefore, would mean more flow turning in the stator.

Parameters at Plane 2 in proximity to the blade's leading edges have steeper gradients, as shown in black in Figure 8 (a). However, the probe "measurements" do follow the trend in both cases, although the offset is not uniform. In the middle pitch the "measured" values are lower, and near the blades are equal or even higher than the local one.

The positions of the stagnation point on the probe's surface are shown for Plane 1 on the same graph in empty circles. When compared against blue squares, an offset of one degree between the probe reading and the stagnation point is seen throughout the pitch, which was explained before as the flow asymmetry on the probe's surface.

In Figure 8 (b) the difference between the undisturbed local flow angle and the "measured" one can reach up to two degrees. But the general trend is still maintained throughout the explored operating range. This is also true for various flow incidences (Figure 8 (c)), although, for high positive incidence the offset is more than two degrees, whereas for high negative incidence this is within a one-degree range.

Figure 9 shows the differences between the probe "readings" and the local values of the flow for the range of operating conditions from Figure 8. Now in Figure 9 the vertical axis shows the difference between the local undisturbed flow and the "measured" one, so zero on the vertical axis means undisturbed flow. For pitch-wise locations between 0.2 and 0.7 the differences between the measured and local flow angles fall closely within a two-degrees range. Therefore, the correction of the probe readings to the local flow values can be less sensitive to the flow conditions, and a simple parabolic correction curve can reduce the probe reading uncertainties to be within a ± 1o range. Beyond this pitchwise region, the probe readings become very sensitive to the flow parameters and the corrections might cause contradictory results.

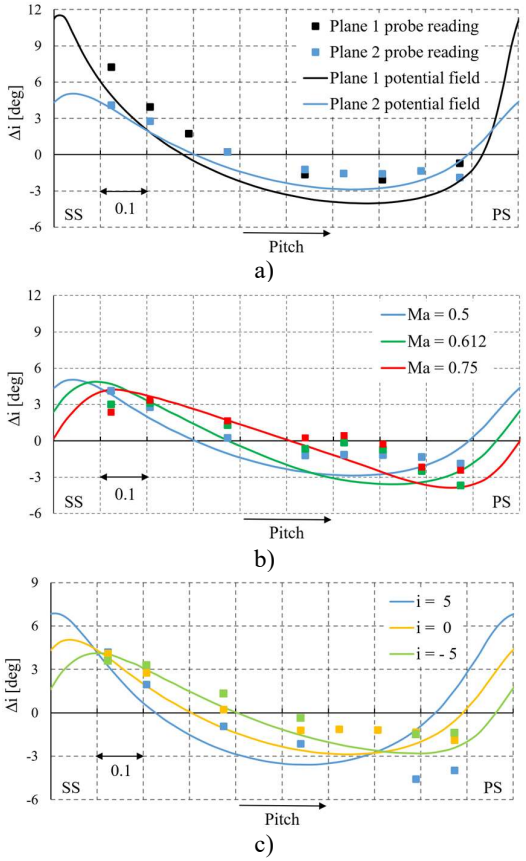

FIGURE 8: FLOW ANGLE AT DIFFERENT PITCHWISE LOCATIONS FOR UNDISTURBED FLOW COMPARED TO PROBE READINGS (ZERO ON VERTICAL AXIS MEANS THE VALUE EQUALS TO THE MASS FLOW AVERAGED): a) FLOW ANGLES AT DIFFERENT AXIAL LOCATIONS, b) AT DIFFERENT MACH NUMBERS, c) AT DIFFERENT INCIDENCES

The reason why the uncertainty region is wider towards the pressure side of the stator than that towards the suction side is in the probe's wake interaction with the blade leading edge. Figure 10 shows the streamlines at the middle pitch (0.4) and far-right – towards the pressure side location of the probe at 5 o incidence and Mach 0.5. In the second case, the wake propagates down to the leading edge of the blade, and depending on the mean flow incidence, this stagnation area can largely affect the velocity distribution and flow symmetry around the probe.

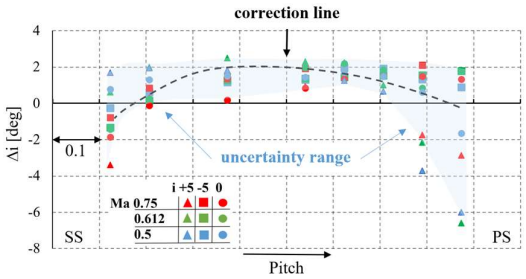

FIGURE 9: FLOW ANGLE DIFFERENCES BETWEEN LOCAL VALUES OF THE UNDISTURBED FLOW AND THE PROBE READINGS AT THE SAME LOCATIONS (ZERO ON THE VERTICAL AXIS MEANS THE LOCAL VALUE OF THE UNDISTURBED FLOW)

Total pressure

For total pressure measurements upstream of the stator, the difference between the "measurements" and the mass flow averaged values did not exceed 1% of the dynamic head within the same pitchwise region as mentioned before for the trustable flow angle "measurements". The reasons for that are also believed to be the same as for the angles. Therefore, the figure showing these differences looks similar to Figure 9 and is omitted here for the sake of the reader's time. The calculations have also proved to be stable within the 20o probe incidence range (see Figure 7).

Static pressure

For static pressure variations the probe blockage plays a major role, and one of the most important factors is the inflow Mach number. In Figure 11 the lines show pitch-wise distributions of the static pressure for several inflow velocities. Zero on the vertical axis means the area averaged static pressure of the undistorted channel. And the points are for the CFD readings of the probe placed at each circumferential position. Here the probe readings are processed using Mach-dependent calibration curves.

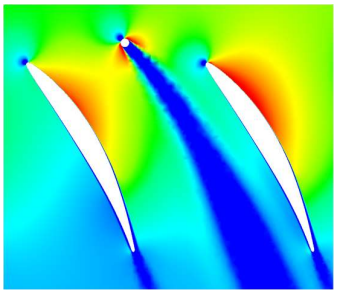

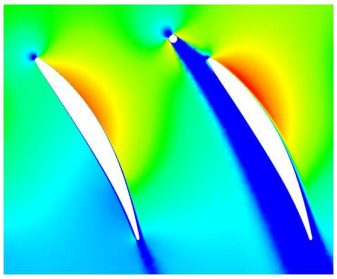

FIGURE 10: FLOW STREAMLINES FOR THE PROBE POSITION AT THE MIDDLE PITCH (TOP) AND IN PROXIMITY TO THE BLADE SUCTION SIDE (BOTTOM). INCIDENCE +5 DEGREES, MACH NUMBER 0.5

Figure 13 shows the distribution of the freestream Cp values at the axial plane of the traverse. The undisturbed flow is presented with a solid line, and the dashed lines of the same colour are for the flow with the probe at one of the locations in mid-pitch. The spike of the Cp to the left and the right of the probe can be seen for both low and high Mach number flows. However, at Mach 0.5 the overall flow field does not change much after three probe diameters away from the probe centre. The channel blockage is causing flow redistribution, which is similar to that reported by Coldrick et al (2003) and Seki et al (2021). For Mach 0.7 the distortion propagates further away toward the neighbouring channels. Therefore, for dynamic head measurements the cylindrical probe has limited performance at Mach numbers above 0.5. Further interpretation of measurement results can be possible at high risk, and it might require an iterative process and consideration of the whole blade height to account for three-dimensional flow redistribution.

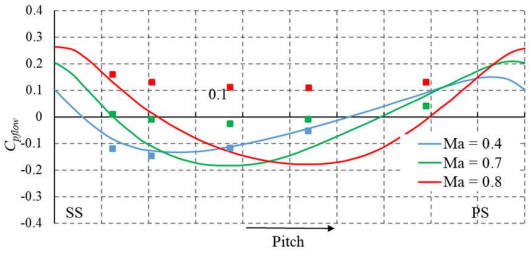

FIGURE 11: Cp VALUES AT DIFFERENT PITCH-WISE LOCATIONS FOR UNDISTURBED FLOW COMPARED WITH PROBE READINGS

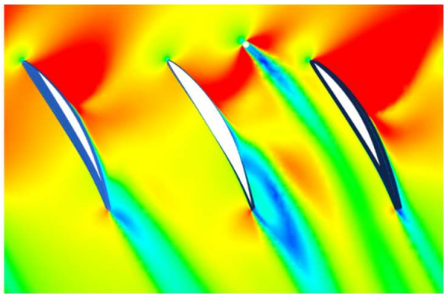

FIGURE 12: MACH NUMBER DISTRIBUTIONS IN THE BLADE CHANNEL WITH THE PROBE FOR THE INLET FLOW MACH Number Of 0.7

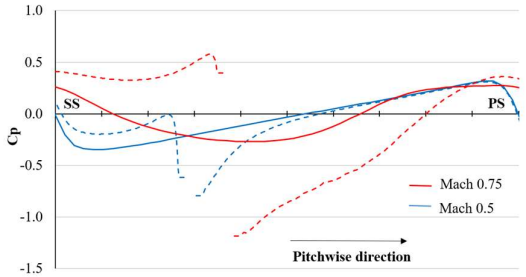

FIGURE 13: PITCH-WISE VARIATIONS OF STATIC PRESSURES FOR UNDISTURBED FLOW AND THE ONE WITH IMMERSED PROBE FOR MACH NUMBERS OF 0.5 AND 0.75

Probe readings downstream of the stator

Figure 14 (a) shows the sample probe position downstream of the stator blades with the readings of angle, total and static pressures shown at (b), (c), and (d) respectively. At the stator exit the potential field has a rather uniform flow distribution along the pitch, so the "measured" values can be referred straight to the flow averaged ones. For the probe positions between 35% and 75% of blade pitch, the readings are consistent and agree with the mass flow averaged value. However, for a high blade incidence, when the separation happens on the suction side of the blade, the effect of probe blockage is more significant, especially in proximity to the suction side, as it improves the local diffusion factor and pushes the flow towards the separation area. For unseparated flows, the measured yaw is between one to four degrees more towards the axial direction, however, for the probe position at 95% of span towards the pressure side the flow angle, and therefore, flow turning would be underestimated. A similar effect was shown by Aschenbruck et al (2015) when measuring the outlet flow of the turbine vane in proximity to the wake. The presence of the probe causes the local flow to turn towards the wake and this affects the measured values.

For the total pressure within the mid-pitch the uncertainty of the readings is within 2.5% of the dynamic head for cases with the unseparated flow. For the same cases the dynamic head uncertainty is within 5%. However, the trustable region for the static pressure is somewhat wider than that for the total pressure

DISCUSSION

The corrections for probe readings can now be discussed. This can be done in the same sequence as the raw data of three-hole pressure probe readings is processed: first, the yaw angle, then the stagnation pressure and the dynamic head [17].

Flow angle measurements follow the general trend of the potential field around the blade leading edges. It was found that the differences between the readings and the local flow angles at the probe location are less dependent on the flow condition, and all the points fall into the narrow region. When comparing against the averaged value, the difference can reach up to 10o. Therefore, processing the measured values of the flow angles as the local ones is more universal. The parabolic correction curve with the central point at 50% of pitch and -2o and branches reaching -0.5o at 20% and 70% of pitch can be used. In that case for the 20-70% of pitch, the measurement uncertainty can be expected within ±1o from the local value of the flow angle. This is found to be the case for all the probe locations and flow regimes studied.

Flow angle measurements downstream of the stator blade row agree with the mass flow averaged values of the undisturbed flow within 4o interval for the 15..75% of the pitch. Again, a parabolic correction curve can be applied with its top at around 35% of pitch and +2o towards a more axial direction.

After correcting the reading to the local flow value, the latter should then be referred to as a representative pitchwise average number. As the local flow distribution upstream of the stator is mainly caused by the potential field, the correction from local to mean flow value can be done by CFD simulation in the same way as coloured lines refer to the zero value in Figure 8.

Downstream of the stator the potential field is weaker, and the gradients in the flow are not that significant. However, attention must be paid to avoid interaction with the wake and the suction side boundary layer, especially in cases of high incidence.

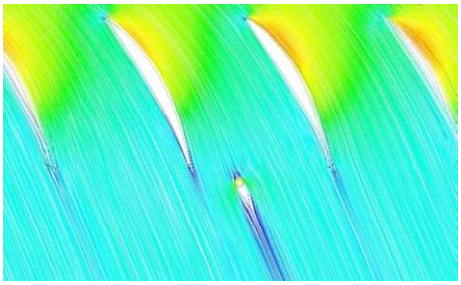

a)

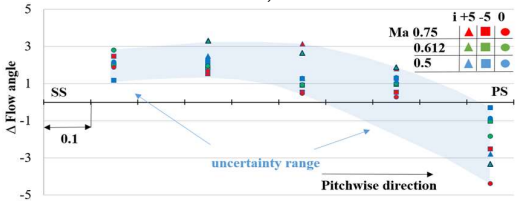

b)

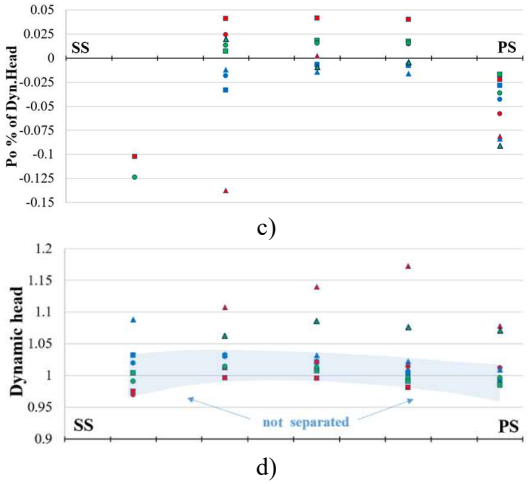

FIGURE 14: PROBE MEASUREMENTS DOWNSTREAM OF THE STATOR BLADE ROW: SCHEMATIC (a), FLOW ANGLE (b), TOTAL PRESSURE (c), STATIC PRESSURE (d)

Total pressure readings in front of the stator blades show a pitchwise uniformly scatter of ±1% deviations between mass flow averaged values and the probe readings. This is rather expected, since the middle hole of the three-hole pneumatic probe, which is mainly responsible for the total pressure value, is located upstream of all the loss sources in the model. At the stator exit the blade boundary layers interfere with the immersed probe, and therefore the flow with and without the probe can only be compared for the middle pitch – from 35% to 75%. The uncertainty range for unseparated flow conditions is within ± 2.5% of the dynamic head. It is also important to notice that the core flow in the blade channel has relatively low losses, so the measured total pressure will be close to that of the stator inlet.

Static pressure readings, or the dynamic head, are found to be sensitive to the flow Mach number. Below Mach number of 0.5, the measured values follow the general trend of the potential field. The difference is consistent and causes about 5-15% lower dynamic head compared to the undisturbed flow. An appropriate correction could reduce the uncertainty in measured values down to 3-5%. At higher flow speeds the probe blockage significantly grows and affects not just the blade channel, where the probe is immersed, but also the neighbouring channels. The dynamic head, therefore, is underestimated by more than 30%. Also, under these conditions the differences are more uniform along with the pitch.

Therefore, measurement corrections can be done in two ways: for low-speed flows the values can be related to the local values of the undisturbed flows, and for the flows with the Mach number of more than 0.5 the corrections of up to 20..30% can be applied pitchwise uniformly, although, this can rather be used for estimation purposes than for precise comparisons.

Presented results are based on the standard thickness distribution airfoils, namely the NACA-65 series, so the data can be cross-checked by other scholars. When a similar exercise was carried out for the proprietary series of blade shapes, similar trends were obtained, which proves the universality of the proposed approach but not of the absolute values. Especially for the stator outlet, attention should be paid to placing the probe outside possible separation regions, typical for a given airfoil.

The reasons why the measured values can be different from those of the undisturbed flow can be summarized as follows:

- proximity to the blade surface generates extra acceleration and shifts the separation point further down the circumference of the cylindrical probe. This leads to a misprediction of the flow angle and the dynamic head, especially at high incidences. It also introduces flow asymmetry to the probe, further affecting the yaw measurements.

- flow acceleration behind the probe also affects the separation point on its surface and the Cp distribution along the circumference, so if one of the probe holes is affected, the freestream calibration curves can no longer be reliably used.

- the probe in the flow acts not just as a blockage, but also causes the local flow to turn more on the side between the cylinder stagnation point and the suction side of the neighbouring blade, and opposite on the other side. This also depends on the proximity of the probe to either side of the inter-blade channel and the passage entrance. It is also a function of compressibility effects.

- the high-uncertainty region is expected to be wider from the pressure side due to the probe's wake interaction with the leading edge of the blade,

- at the stator outlet the probe also affects the boundary layer behaviour and the trailing edge wake, so the local flow angle can be far off from the mass averaged one.

Important to notice here that the probe size plays a critical role in the flow field interaction, and for a half-sized probe the uncertainties were less than 0.8o for the local flow angle. However, such a small relative diameter was not technologically feasible in this study, and the aerodynamically insensitive relative probe size can be a subject for further research.

Considering the trend towards higher pressure ratios and smaller blades, it can be expected that nondimensional probe size is rather likely to increase. As a result, more attention should be paid to processing and interpreting experimental data.

For the spanwise traversing results the corrections were applied accordingly, and Figure 15 shows the experimentally measured values of the integrated mass flow with applied corrections for different sections of the industrial compressor. The axial Mach number distributions at two different sections are presented as an example. Empty

symbols are given for the raw processed values and the solid ones are for the corrected ones. For reference, the orange line represents the CFD results at the same section and same inlet mass flow conditions. By no means CFD results could be treated here as the "true" values that one should aim for, but it is the case, that the CFD can maintain mass conservation throughout the whole computational model, and, since the inlet mass flow is taken from experiment, then the rest of the sections should give the same value, and axial flux from the experiment can be compared to that of the computation. In Figure 15 the measured axial Mach number is about 5 to 10% higher than that of the CFD. But for later stages the spanwise blockage distribution, predicted by CFD simulation of the compressor, is even higher, therefore the difference in integral mass flow would be larger.

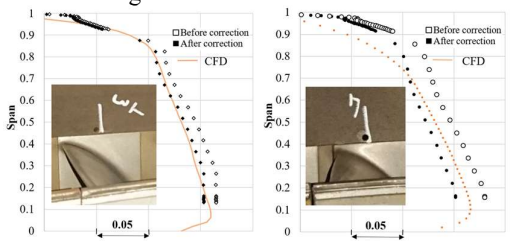

FIGURE 15: SPANWISE DISTRIBUTION OF THE AXIAL FLOW MACH NUMBER AT TWO DIFFERENT COMPRESSOR SECTIONS

As can be seen in the photos of the probe holes (marked white in Figure 15), the probe locations here are at about 35% and 25% of pitch respectively, measured from the blade suction side. So, according to Figure 12 for the Mach number of 0.5 and below the overestimation of the dynamic head could be up to 15% of the pitchwise averaged value, and up to 5% underestimation compared to the local one.

Since the blades at these compressor stages have a constant spanwise profile with the radially aligned leading edge, a similar level of corrections was applied along the radius.

As a result, solid symbols on the graphs show improvement in the axial flow speed. On the left-hand side, the spanwise blockage is matching well for both simulation and the measurements, and after the correction, the axial Mach number distributions also fall in good agreement, apart from the hub region. On the right-hand side, the axial Mach number at midspan is lower than that of the CFD, which together with lower spanwise blockage in the experiment gives agreement in the mass flow estimations.

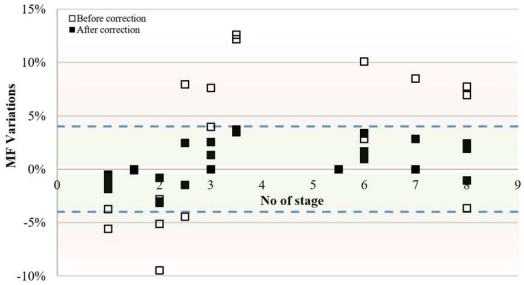

FIGURE 16: MASS FLOW VARIATIONS AT DIFFERENT SECTIONS OF THE COMPRESSOR BEFORE AND AFTER CORRECTION

Figure 16 shows significant improvement in variations of the integrated mass flow values for all the sections. The spread of the mass flow values within 4% is still fairly high for the idealized laboratory experimentation, however, for the given compressor this can be explained mainly by the lack of measurement points in the hub region together with high measurement uncertainties near both of the end walls. An undefined shape of the axial velocity spanwise profile in these regions was found to be the largest contributor to the uncertainty. For this study, the shape of the missing part of the experimental spanwise profile was taken parallel to the one from CFD with the offset of the last measured point. Since the missed readings were in the hub section, the impact on the total mass flow was relatively low, and the estimations with variable profile extrapolations have shown up to 5% uncertainty in total mass flow.

CONCLUSION

A computational study has been carried out to assess the effect of the flow field interaction between the stator blades and the pneumatic probe on the probe's readings. The simulations were made within the range of flow conditions, representative of real industrial gas turbine engines.

When the pneumatic probe is immersed upstream of the stator, it measures the flow's local parameters. The difference with representative pitchwise average values is mainly caused by the potential flow field effect, which can be accounted for by doing CFD simulation. However, the measured parameters cannot be treated as true local values since the flow is further complicated by the presence of the probe. The differences between the actual value of the flow and the probe reading can be significant and they can be nonlinear depending on the probe circumferential location and inlet flow conditions.

The main factors causing these uncertainties are:

- the flow asymmetry around the probe with extra acceleration on one of the sides when it is approaching the suction side of the blade,

- downstream flow distortion when the probe is approaching the pressure side of the blade and its leading edge,
- the asymmetry around the probe due to the flow gradient in pitchwise direction and the finite size of the probe, so the sides are exposed to different freestream conditions,
- the interaction with the boundary layer and the wake when measuring downstream of the stator.

To minimize the measurement uncertainties the designer should aim for the middle of the pitch – a region of 20 to 70% was shown to have a narrow spread of the readings in the whole range of explored flow conditions. This could simplify the correction procedure for the measured data. For measurements downstream of the stator similar range can be considered, providing the blade is not separated.

Special attention should be paid to high Mach number cases when the uncertainty in dynamic head estimation grows rapidly. For downstream measurements the critical conditions are the high-incidence/high-separation flows when the immersed probe is interacting with the separated boundary layer and significantly changes the flow.

Presented results should help designers make informed decisions about compressor instrumentation, particularly the circumferential position of the traversing gear and the good practice for processing the acquired experimental data.

What remains beyond the scope of the present work is the probe behaviour in proximity to the end walls, where the experimental data had shown reasonable agreement with theoretical expectations and computational results, but the uncertainty of these readings remains to be understood and quantified.

ACKNOWLEDGEMENTS

Put acknowledgements here.

REFERENCES

[1] Dransfield, D. C., and Calvert W. J., 1976, "Detailed flow measurements in a four-stage axial compressor." ASME paper 76-GT-46.

[2] Tweedt D.L., Okiishi T.H., 1983, "Stator Blade Row Geometry Modification Influence On Two-Stage, Axial-Flow Compressor Aerodynamic Performance," Technical report AD-A141 793.

[3] Lakshminarayana, B. & Suryavamshi, N. & Prato, J. & Moritz, R., 1996, "Experimental Investigation of the Flow Field in a Multistage Axial Flow Compressor". International Journal of Rotating Machinery. 2. 10.1155/S1023621X96000127.

[4] Ikeguchi, T, Matsuoka, A, Sakai, Y, Sakano, Y, & Yoshiura, K., 2012, "Design and Development of a 14-Stage Axial Compressor for Industrial Gas Turbine" Proceedings of the ASME Turbo Expo 2012: Turbine Technical Conference and Exposition. Volume 8: Turbomachinery, Parts A, B, and C. Copenhagen, Denmark. June 11–15, 2012. pp. 125-134. ASME.

[5] He X., Ma H., Ren M., Xiang H., 2012, "Investigation of the Effects of Airfoil-probes on the Aerodynamic Performance of an Axial Compressor," Chinese Journal of Aeronautics 25, pp. 517-523.

[6] Ng H., Coull J.D., 2017, "Parasitic Loss Due to Leading Edge Instrumentation on a Low-Pressure Turbine Blade," J. Turbomach. Apr 2017, 139(4): 041007.

[7] Lecheler, S, Schnell, R, & Stubert, B., 2001, "Experimental and Numerical Investigation of the Flow in a 5-Stage Transonic Compressor Rig," Proceedings of the ASME Turbo Expo 2001: Power for Land, Sea, and Air. Volume 1: Aircraft Engine; Marine; Turbomachinery; Microturbines and Small Turbomachinery. New Orleans, Louisiana, USA. June 4–7, 2001. V001T03A040. ASME.

[8] Coldrick S., Ivey P., Wells R., 2003, "Considerations For Using 3-D Pneumatic Probes In High-Speed Axial Compressors," J. Turbomach. Jan 2003, 125(1): 149-154.

[9] Coldrick, S, Ivey, PC, & Wells, RG., 2004, "The Influence of Compressor Aerodynamics on Pressure Probes: Part I — In Rig Calibrations," Proceedings of the ASME Turbo Expo 2004: Power for Land, Sea, and Air. Volume 2: Turbo Expo 2004. Vienna, Austria. June 14–17, 2004. pp. 509-514. ASME.

[10] Aschenbruck J., Hauptmann T., Seume J. R., 2015, "Influence Of A Multi-Hole Pressure Probe On The Flow Field In Axial-Turbines," Proceedings of 11th European Conference on Turbomachinery Fluid dynamics & Thermodynamics ETC11, March 23-27, 2015, Madrid, Spain.

[11] Seki R., Yamashita S., Mito R., 2021 "Evaluation of a Flow Measurement Probe Influence on the Flow Field in High-Speed Axial Compressors" Proceedings of ASME Turbo Expo 2021 (online), 7-11 June 2021. ASME Paper No. GT2021-58558.

[12] Zhong, Y, Ma, H, & Yang, Y., 2021, "Effects of Probe Stem Surface Suction on the Aerodynamic Performance of a Compressor," Proceedings of the ASME Turbo Expo 2021: Turbomachinery Technical Conference and Exposition. Volume 2A: Turbomachinery — Axial Flow Fan and Compressor Aerodynamics. Virtual, Online. June 7–11, 2021. V02AT31A024. ASME. GT2021-59047

[13] Mito R., Walker T., Hamana H., Gao X., Sakamoto Y., 2015, "Computational Fluid Dynamics Technology Applied to High Performance, Reliable Axial Compressors for Power Generation Gas Turbines," Mitsubishi Heavy Industries Technical Review Vol. 52 No. 1.

[14] Kupferschmied P., 1998, “Zur Methodik zeitaufgelöster Messungen mit Strömungssonden in Verdichtern und Turbinen”, ETH dissertation No. 12774, Zürich, Switzerland.

[15] Munivenkatareddy S., Sitaram N., 2016, “Extended Calibration Technique of a Four-Hole Probe for Three-Dimensional Flow Measurements,” Hindawi Publishing Corporation International Journal of Rotating Machinery Volume 2016, Article ID 5327297.

[16] Zhang D., Cheng L., An H., Draper S., 2020, “Flow Around A Surface-Mounted Finite Circular Cylinder Completely Submerged Within The Bottom Boundary Layer,” European Journal of Mechanics, B Fluids 86 (2021), pp. 169–197.

[17] Chasoglou A.C., Mansour M., Kalfas A.I., Abhari R. S., 2018, “A Novel 4-Sensor Fast-Response Aerodynamic Probe For Non-Isotropic Turbulence Measurement In Turbomachinery Flows,” Journal of the Global Power and Propulsion Society.2, pp. 362–375.